nature structural & molecular biology

SMG6 promotes endonucleolytic cleavage of nonsense mRNA in human cells

Andrea B Eberle[1,3], Søren Lykke-Andersen[2,3], Oliver Mühlemann[1,4] & Torben Heick Jensen[2,4]

From yeast to humans, mRNAs harboring premature termination codons (PTCs) are recognized and degraded by nonsense-mediated mRNA decay (NMD). However, degradation mechanisms of NMD have been suggested to differ between species. In *Drosophila melanogaster*, NMD is initiated by endonucleolysis near the PTC, whereas in yeast and human cells the current view posits that NMD occurs by exonucleolysis from one or both RNA termini. Here we report that degradation of human nonsense mRNAs can be initiated by PTC-proximal endonucleolytic cleavage. We identify the metazoan-specific NMD factor SMG6 as the responsible endonuclease by demonstrating that mutation of conserved residues in its nuclease domain—the C-terminal PIN motif—abolishes endonucleolysis *in vivo* and *in vitro*. Our data lead to a revised mechanistic model for degradation of nonsense mRNA in human cells and suggest that endonucleolytic cleavage is a conserved feature in metazoan NMD.

© 2008 Nature Publishing Group http://www.nature.com/nsmb

There are numerous RNA quality control systems in eukaryotic cells to ensure a sufficiently high accuracy of expression of genetic information[1]. Among these, NMD represents a surveillance process that protects cells from the synthesis of potentially deleterious C-terminally truncated polypeptides through recognition and degradation of mRNAs harboring PTCs[2–5]. In addition to its quality control function, NMD also constitutes a translation-dependent post-transcriptional pathway to regulate the expression levels of alternatively spliced mRNAs, of mRNAs with upstream open reading frames (uORFs), and of mRNAs with long 3′ untranslated regions (3′ UTRs) or with introns in the 3′ UTR[6–8]. Genome-wide transcriptome-profiling analyses of the budding yeast *Saccharomyces cerevisiae*, *D. melanogaster* Schneider cells and human tissue culture cells have revealed that 3–10% of all mRNAs are affected by NMD[9–12]. In yeast, about half of these transcripts have been identified as direct NMD targets[13]. Finally, with an estimated 30% of all known human disease–associated mutations generating a nonsense mRNA, NMD also serves as an important modulator of genetic disease phenotypes[14].

With regard to the mechanism of NMD, recent progress has been made toward understanding how cells recognize and distinguish PTCs from correct stop codons[15–21]. Via its strict coupling to active translation[2,22], NMD can 'sense' PTCs because they generally lead to inefficient translation termination with consequential ribosome stalling[15]. The reason for this poorly dissociable termination complex seems to be the absence of a termination-stimulating signal that requires the interaction between the poly(A) tail binding protein and ribosome-bound eukaryotic release factor 3 (eRF3) (reviewed in refs. 2,5). Consistent with this 'faux 3′ UTR' model, the physical distance between the terminating ribosome and the poly(A) tail was identified as an important determinant for PTC recognition[8]. The model further posits that NMD ensues in the absence of the termination-stimulating signal by a competing interaction of eRF3 with the essential and conserved NMD factor UPF1. This in turn allows ribosome-bound UPF1 to be activated and congregate other components of the NMD machinery. Rather than being a prerequisite for PTC definition, the presence of an exon junction complex (EJC) downstream of the termination codon serves as an enhancer of mammalian NMD according to this model (reviewed in ref. 5).

In contrast to PTC recognition, little is known about the mechanisms that trigger the rapid degradation of mammalian nonsense mRNA. Previous reports have suggested that, similarly to NMD in budding yeast[23–25], it may occur through the general mRNA-turnover pathway, involving deadenylation, decapping and subsequent exonucleolytic degradation[26–29]. However, the relative contributions of different mRNA degradation pathways to NMD cannot be easily determined by currently used experimental approaches, because different pathways might be redundant (if one is blocked another may take over) or may not be independent (depletion of a component of one pathway may also affect another). Perhaps most importantly, it is not trivial to determine whether true NMD is being measured, that is, to discriminate between the fraction of transcripts going through the NMD pathway and the fraction escaping NMD and being degraded by 'normal' mRNA-decay pathways. Finally, the unstable nature of RNA-degradation intermediates further complicates delineation of the exact degradation pathway(s) at play. The last point is illustrated by evidence that degradation of nonsense mRNA in *D. melanogaster* cells is initiated by an endonucleolytic cleavage. This evidence has been obtained under conditions where

[1]Institute of Cell Biology, University of Bern, Baltzerstrasse 4, CH-3012 Bern, Switzerland. [2]Centre for mRNP Biogenesis and Metabolism, Department of Molecular Biology, Aarhus University, C.F. Møllers Alle, Building 1130, 8000 Aarhus, Denmark. [3]These authors contributed equally to this work. [4]Correspondence should be addressed to T.H.J. (thj@mb.au.dk) or O.M. (oliver.muehlemann@izb.unibe.ch).

Received 6 November; accepted 18 November; published online 7 December 2008; doi:10.1038/nsmb.1530

3′-5′ and 5′-3′ exonucleases were depleted, respectively, facilitating detection of the highly unstable 5′- and 3′-endocleavage products[30].

In this paper, we use a strategy similar to one used with *D. melanogaster* cells to revisit the decay pathways of human nonsense mRNAs. We demonstrate a previously unobserved, substantial contribution of endonucleolysis to NMD in both HEK293 and HeLa cells. Moreover, we identify the metazoan-specific NMD factor SMG6 as the responsible endonuclease. Our data revise the current model for PTC-triggered turnover of human nonsense mRNA.

RESULTS

Depletion of exonucleases reveals PTC-specific mRNA fragments

To test whether NMD in human cells can also be initiated by endonucleolysis, we established RNAi-mediated knockdown protocols in HEK293 and HeLa cells of the 5′-3′ exonucleases XRN1 and XRN2, the decapping enzyme DCP2, the EXOSC1 (human homologue of yeast Csl4), EXOSC2 (homologue of Rrp4), EXOSC4 (homologue of Rrp41), SKIV2L (homologue of Mtr4 or Ski2) and WDR61 (homologue of Ski8) components of the 3′-5′ exonucleolytic RNA exosome, and as a positive control the bona fide NMD factor UPF1 (**Supplementary Fig. 1a–e** online). Under single or double knockdown conditions, we assayed steady-state levels of two different stably expressed NMD reporters by northern blotting analysis: a β-globin transcript containing a PTC after codon 39 (β 39) and a TCR-β minigene transcript harboring a PTC at codon 68 (TCRβ 68) (**Fig. 1**).

As previously described[22,31,32], levels of both nonsense mRNAs were considerably lowered compared to their PTC-free (wild-type) counterparts and, as expected for NMD substrates, this effect was suppressed by knockdown of UPF1 (**Fig. 1c,d**). Notably, however, knockdown of the major cytoplasmic 5′-3′ exonuclease XRN1 did not lead to markedly increased levels of full-length PTC-containing reporter transcripts, but instead we observed a faster-migrating species that was not detected with the PTC-free constructs. These smaller RNA fragments were detected with probes targeting the full-length mRNAs (data not shown) or the 3′ regions downstream of the respective PTCs, but not with probes targeting 5′ regions upstream of the PTC (**Fig. 1c,d**).

A β 39 3′ fragment generated by oligonucleotide-directed RNase H cleavage of the mRNA at the PTC was a similar size to the β 39

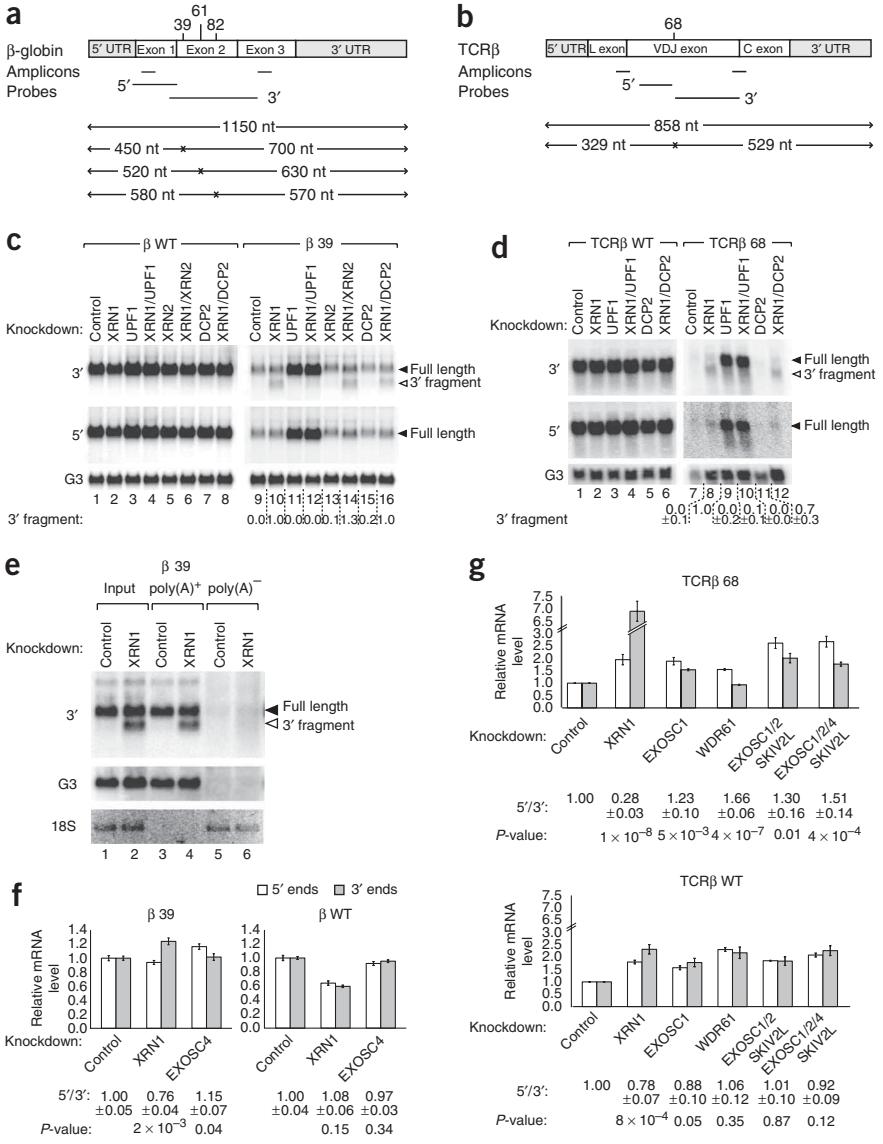

Figure 1 Distinct 3′ and 5′ fragments are produced from nonsense mRNA upon depletion of exonucleases. (**a**,**b**) Schematic representation of the β-globin (**a**) and TCRβ (**b**) reporter mRNAs used in this study, which were stably expressed in HEK293 and HeLa cells, respectively. The positions of the PTCs are indicated above the mRNA. ORFs are depicted in white, 5′ and 3′ UTRs in gray, and exon-exon junctions as black vertical lines. Positions of riboprobes used for northern analyses and amplicons generated by qPCR, as well as expected sizes of endocleavage products, are shown below the constructs. (**c**,**d**) Northern blotting analysis of total RNA isolated from HEK293–β-globin wild-type (β WT) or HEK293–β-globin 39 (β 39) (**c**) or HeLa–TCRβ wild-type (TCRβ WT) or HeLa–TCRβ 68 (TCRβ 68) (**d**) cell lines depleted for the indicated factors. The blots were hybridized with probes directed against the 3′ or 5′ regions of the respective reporter RNA. GAPDH (G3) levels were detected as an internal loading standard. Relative 3′ fragment levels of the PTC-containing constructs were quantified by subtracting the background signal of the full-length transcripts. For TCRβ 68, mean values with standard errors were calculated ($n = 3$). 3′ fragment levels in the XRN1 knockdowns were set to 1. (**e**) Northern blot analysis of oligo-dT–selected RNA isolated from the β 39 cell line submitted to either control or XRN1 knockdown. GAPDH (G3) and 18S rRNA (18S; detected by ethidium bromide staining of the gel) served as controls. (**f**,**g**) RT-qPCR measurements of 5′ and 3′ ends of the β 39 and β WT (**f**) and TCRβ 68 and TCRβ WT (**g**) reporters isolated from cells depleted for the indicated exosome components or XRN1. The relative amounts of the 5′ and 3′ amplicons obtained from the knockdown experiments were normalized to the corresponding values of the control knockdown. *P*-values were determined using a two-tailed paired student's *t*-test ($n = 3$ in **f**; $n = 4$ in **g**).

© 2008 Nature Publishing Group http://www.nature.com/nsmb

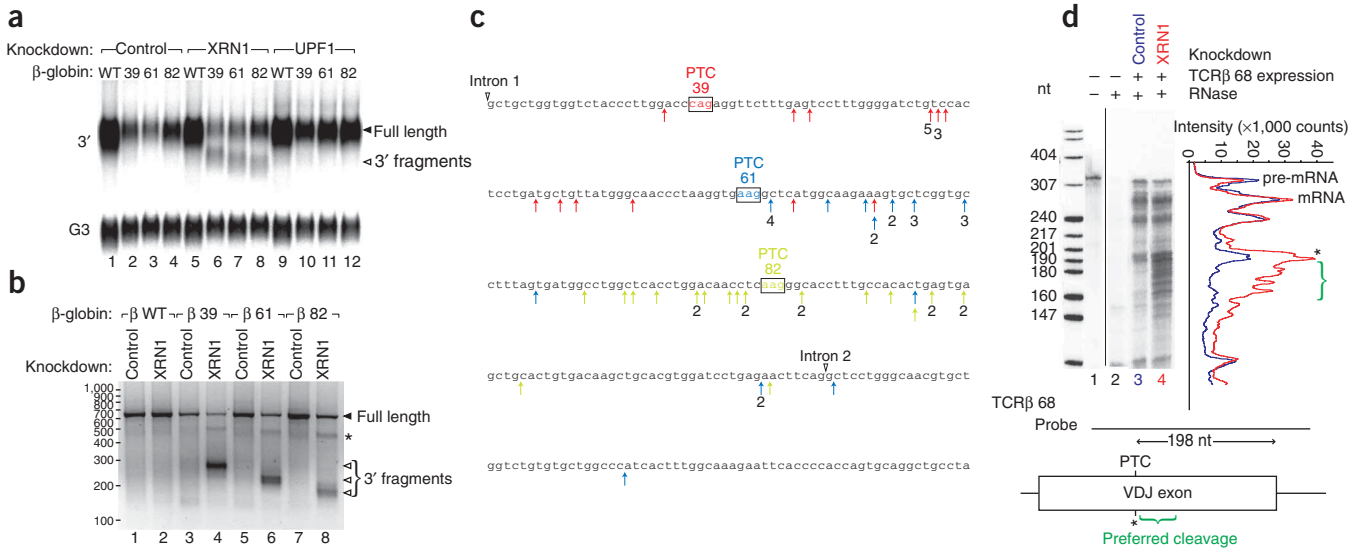

Figure 2 Sizes of the 3′ end decay intermediates correlate with the position of the PTC. (**a**) Northern blot analysis of total RNA isolated from HEK293–β-globin WT, 39, 61 or 82 cell lines depleted for the indicated factors. The blot was hybridized with probes directed against the 3′ end of the β-globin mRNA and GAPDH (G3). (**b**) Agarose gel visualizing 5′ RACE products of the XRN1 depletion–specific 3′ fragments obtained after endocleavage of β 39, β 61 and β 82 reporter RNAs. Migrations of 5′ RACE products reflecting full-length RNAs and 3′ fragments are indicated. An asterisk denotes putative hybrid DNA. (**c**) Excerpt of the β-globin ORF with a summary of the detected 5′ ends for the three tested PTCs. Arrows (β 39 in red, β 61 in blue and β 82 in green) indicate positions of 5′ ends as determined by sequencing of individual clones obtained from 5′ RACE. The numbers below the arrows indicate the number of clones with a 5′ end at that particular position. Exon-exon junctions are indicated by white arrowheads. A total of 18, 22 and 22 clones were sequenced for β 39, β 61 and β 82, respectively. (**d**) RNase protection assay of TCRβ 68 RNA (above left). Total RNA, isolated from HeLa-TCRβ 68 cells subjected to control or XRN1 knockdown as indicated, was hybridized with a ^{32}P-labeled riboprobe spanning a region upstream of the PTC in the VDJ exon into the downstream intron (below). RNA from HeLa cells devoid of the TCRβ reporter served as a specificity control (lane 2) and a control for nonspecific degradation of the probe (lane 1). Protected fragments after RNase digestion were separated on a denaturing polyacrylamide gel. Signal-intensity profiles down through lanes 3 and 4 are shown (above right) with the position of the PTC denoted with an asterisk.

3′ fragment seen upon depletion of XRN1 (data not shown), suggesting that the latter represents the 3′ product of an endonucleolytic cleavage event in the vicinity of the PTC. Further supporting this idea, the β 39 3′ fragment was detected in the poly(A)$^+$ but not in the poly(A)$^-$ RNA fraction, demonstrating that it is polyadenylated (**Fig. 1e**). Notably, when XRN1 and UPF1 were codepleted, the β 39 3′ fragment was no longer produced, showing that the putative endonucleolytic event occurred as part of the NMD process downstream of UPF1 action (**Fig. 1c**). For TCRβ 68, some signal in the range of the 3′ fragment persisted in the XRN1 and UPF1 double knockdown, but probing with the 5′ probe and quantification of the data revealed that this mainly represents full-length RNA (**Fig. 1d**), a conclusion fully supported by 5′ rapid amplification of cDNA ends (5′-RACE) analysis of the relevant TCRβ samples (**Supplementary Fig. 1f**). As decapping is a prerequisite for 5′-3′ decay of full-length transcripts, it is noteworthy that the levels of the β 39 and TCRβ 68 3′ fragments were unchanged when DCP2 was codepleted with XRN1 (**Fig. 1c**,**d**). With the caveat that residual DCP2 activity may persist despite the efficient knockdowns (**Supplementary Fig. 1a**,**b**), this observation further supports the notion that the 3′ fragments result from endonucleolytic cleavage rather than from decapping followed by residual XRN1 or 'non-XRN1' 5′-3′ exonucleolytic activity.

In addition to the endonucleolytic 3′ products, we also attempted to detect the corresponding 5′ products by RNA interference (RNAi)–mediated depletion of several RNA exosome subunits, including the catalytically active DIS3 (also known as RRP44) and EXOSC10 (RRP6) components, individually and in different combinations (**Supplementary Fig. 1c–e** and data not shown). Similarly to the case in *D. melanogaster* cells[30], it was difficult to stabilize 5′ products from endocleavage reactions, and our efforts to unambiguously detect them by northern blotting analysis were unsuccessful, a result that we attribute to the likely possibility that decay of these fragments is carried out by redundant, including yet to be identified, 3′-5′ exonucleases. However, measurement of relative TCRβ 68 RNA levels upstream and downstream of the PTC by reverse-transcription quantitative PCR (RT-qPCR) revealed a small, but significant, enrichment of 5′ ends over 3′ ends when EXOSC1, EXOSC2, EXOSC4, SKIV2L or WDR61 were depleted together or individually (**Fig. 1g**). Notably, we did not observe this increased 5′/3′ ratio for TCRβ wild-type RNA in these knockdowns. A similar result was obtained for β 39 RNA upon depletion of EXOSC4, which also leads to depletion of additional exosome components[33] (**Fig. 1f**).

Endonucleolytic cleavage occurs near the PTC

We next constructed additional cell lines expressing β-globin with PTCs at different positions in the ORF (**Fig. 1a**, β 61 and β 82). Consistent with endonucleolysis occurring in the vicinity of the PTC, the sizes of the stabilized 3′ fragments changed according to the position of the PTC (**Fig. 2a**). A similar result was obtained with two differently positioned PTCs in an immunoglobulin-μ (Ig-μ) minigene reporter mRNA (**Supplementary Fig. 2** online). To assess the cleavage sites of the β 39, β 61 and β 82 reporter mRNAs more precisely, we sequenced individual clones of 5′-RACE products specifically obtained from these RNAs (**Fig. 2b**). The 5′ ends of the 3′ fragments were mostly in the vicinity of their related stop codons; however, the exact positions varied depending on the specific mRNA (**Fig. 2c**). A similar picture emerged when preferred cleavage sites of the TCRβ 68 RNA were assessed by RNase protection analysis (**Fig. 2d**): compared to the

© 2008 Nature Publishing Group http://www.nature.com/nsmb

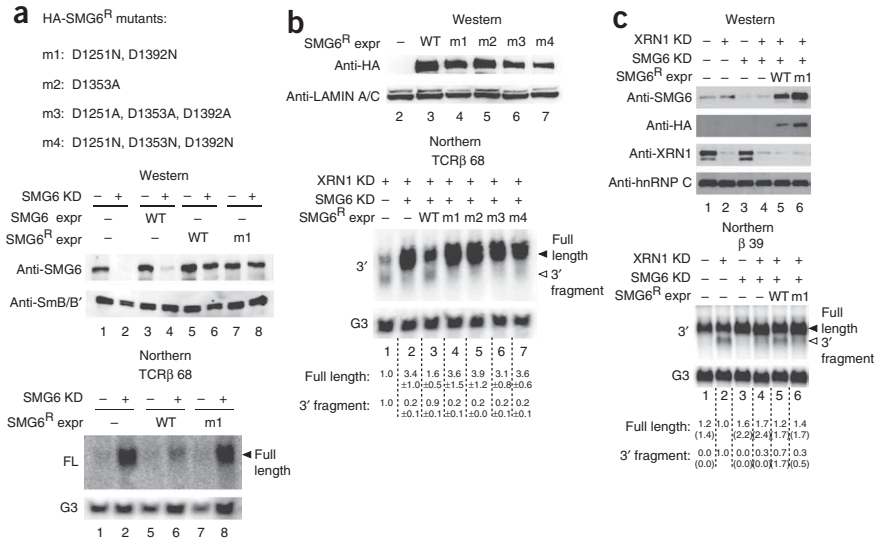

Figure 3 SMG6 induces endocleavage of nonsense mRNA through its PIN domain. (**a**) Above, sequences of the hemagglutinin (HA)–tagged SMG6^R PIN domain mutants (m1-m4) used. Middle, western blotting analysis demonstrating RNAi-mediated knockdown of SMG6 and the ectopic expression of RNAi-resistant HA-tagged versions of SMG6 (wild-type (WT) and m1 HA-SMG6^R) at equal levels in HeLa–TCRβ 68 cells. Below, northern blotting analysis of total RNA isolated from HeLa–TCRβ 68 cells shown in lanes 1, 2, 5, 6, 7 and 8 of the above western blot. The northern blot was hybridized with a probe spanning the VDJ region. (**b**,**c**) Western (above) and northern (below) blotting analyses of material isolated from HeLa–TCRβ 68 (**b**) or HEK293–β 39 (**c**) cells depleted for, and expressing, the indicated factors or mutants. Westerns blots were probed with SMG6- (anti-SMG6 or anti-HA) and XRN1-detecting antibodies as indicated. Anti-SmB/B′, anti–LAMIN A/C and anti–hnRNP C antibodies were used as loading controls. Northern blots were probed as in **Figure 1c**,**d**. For TCRβ 68 (**b**, below) and β 39 (**c**, below) northerns, full-length and 3′ fragment levels were quantified relative to levels in the XRN1 knockdown, as in **Figure 1c**,**d**. For TCRβ 68, mean values with standard errors were calculated ($n = 3$). For β 39, values from two independent experiments are given (values in the above row are from the northern blot shown, whereas the numbers in brackets are from the second experiment). In all experiments (**a**–**c**), matching lane numbering below blots indicate that western and northern analyses were performed on the same cell population.

© 2008 Nature Publishing Group http://www.nature.com/nsmb

protection pattern in the control knockdown, depletion of XRN1 generated a set of additional protected RNA fragments, indicating major cleavage sites between 5 and 40 nucleotides downstream of the PTC. Collectively, these data indicate PTC-proximal endocleavage of all reporters. However, we cannot exclude the possibility that subsequent exonucleolytic 'nibbling' of the products also contributes to the actual 5′ ends detected.

SMG6 is the endonuclease involved in human NMD

Notably, the human NMD factors SMG5 and SMG6 both harbor a C-terminal PIN domain present in many nucleases[34,35]. Although SMG5 and SMG6 share a similar overall RNase fold, only the PIN domain of SMG6 contains the key catalytic residues and shows ribonucleolytic activity *in vitro*[35]. Furthermore, as the X-ray structure of the SMG6 PIN domain is similar to the structure of the catalytic domain of bacteriophage T4 endonuclease RNase H[35], we decided to test whether SMG6 is involved in endocleavage of our NMD reporters.

To this end, we used RNAi to deplete the endogenous pool of SMG6 and replaced it, via plasmid transfection, with recombinant hemagglutinin (HA)–tagged RNAi-immune SMG6 (**Fig. 3**, HA-SMG6^R). Of the recombinant SMG6, we expressed either the functional wild-type form or mutants m1–m4, in which one or several of the three conserved aspartate residues (Asp1251, Asp1353 and Asp1392) in the catalytic center of the PIN domain[35] were changed into asparagine or alanine (**Fig. 3a**, above). Whereas decreased expression of RNAi-sensitive recombinant SMG6 was detected in the background of the SMG6 knockdown, endogenous SMG6 could be replaced with both wild-type and mutant HA-SMG6^R (**Fig. 3a–c**). Under these conditions, wild-type HA-SMG6^R restored NMD of TCRβ 68 and to a lesser extent of the β 39 reporter, as evidenced by the reduced levels of full-length transcript (**Fig. 3a**, compare lanes 2 and 6; **Fig. 3b**, compare lanes 2 and 3; **Fig. 3c**, compare lanes 4 and 5). In contrast, none of the HA-SMG6^R mutants restored NMD. Notably, when taking advantage of the XRN1-depletion context, knockdown of SMG6 diminished the detection of the TCRβ 68 and β 39 3′ fragments, demonstrating their SMG6 dependence (**Fig. 3b**,**c**). Production of the 3′ fragments was reestablished in cells expressing wild-type HA-SMG6^R, but not by the HA-SMG6^R mutants. The failure of the HA-SMG6^R mutants to restore 3′ fragment generation reflects intrinsic features of the PIN domain, because wild-type and mutant recombinant HA-SMG6^R both localized correctly to the cytoplasm (**Supplementary Fig. 3a** online) and co-immunoprecipitated UPF1 with the same efficiency (**Supplementary Fig. 3b**). Thus, our data strongly suggest that the PIN domain of SMG6 is directly involved in endonucleolytic cleavage of PTC-containing RNAs in human cells.

We obtained direct evidence that SMG6 is an endonuclease by *in vitro* experiments with recombinant SMG6 PIN domains produced in *Escherichia coli*. The wild-type PIN polypeptide, but not its D1353A mutant counterpart, was able to cleave a circular RNA (**Fig. 4**). The inactivity of the D1353A mutant confirms

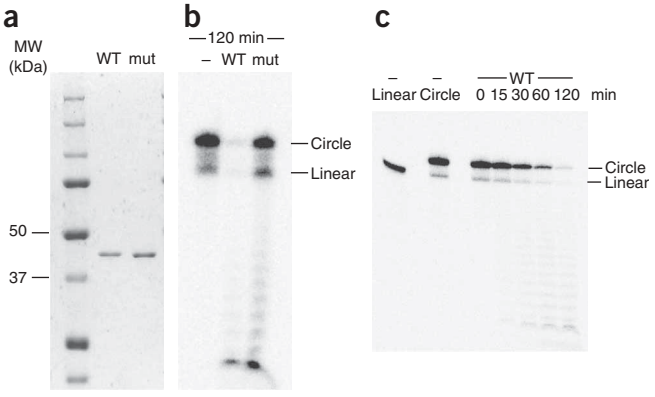

Figure 4 The PIN domain of SMG6 can cleave a circular RNA. (**a**) Purified recombinant GST–SMG6-PIN wild type (WT) and mutant (mut) PIN (D1353A) were analyzed by SDS-PAGE, followed by Coomassie staining. (**b**) Wild-type or mutant protein was incubated with circular ^{32}P-labeled RNA for 120 min and analyzed on 20% PAGE. (**c**) Cleavage pattern of wild-type SMG6 PIN domain over time. Linear RNA and circular RNA without protein served as controls.

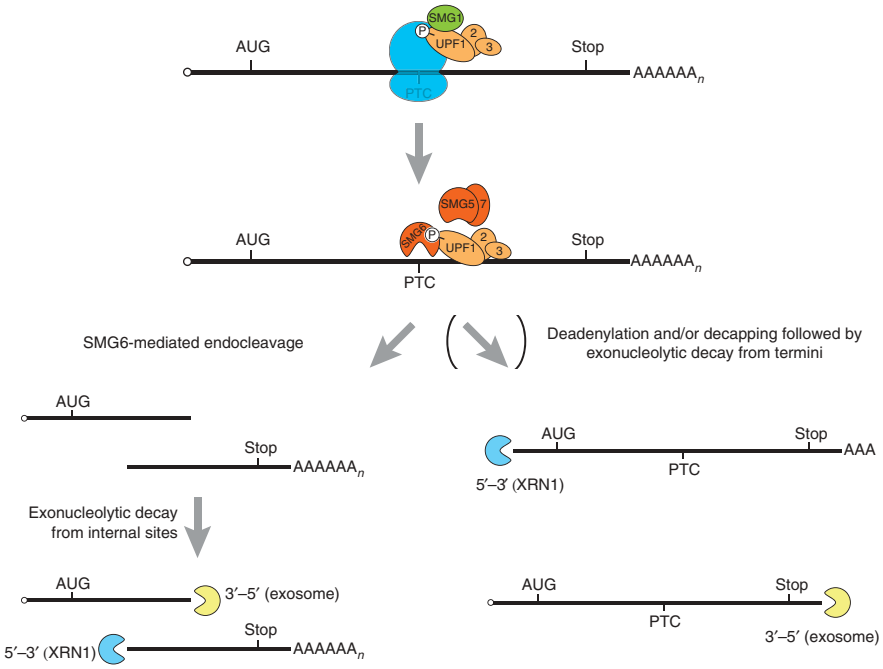

Figure 5 Model for NMD in mammals. The ribosome is depicted in blue, SMG1 in green, UPF1, UPF2 and UPF3 in orange, SMG5, SMG6 and SMG7 in red, and XRN1 and the exosome as blue and yellow pacman shapes, respectively. Parentheses indicates the unclear utilization of exonucleolysis in human NMD. See text for details.

that the observed endocleavage activity resides in the RNase H fold of the SMG6 PIN domain, rather than originating from a contaminating *E. coli* endonuclease.

DISCUSSION

This paper documents evidence that NMD in human cells can be initiated by a SMG6-mediated endonucleolytic cleavage of the nonsense mRNA near the PTC. Corroborating our findings, SMG6 has recently also been identified as the responsible endonuclease in NMD in *D. melanogaster* S2 cells[36]. Together, these data strongly indicate that SMG6-mediated endonucleolytic cleavage is a conserved feature in metazoan NMD. Furthermore, the similar PIN motif of the yeast RNA exosome component Dis3 (also known as Rrp44) has recently been shown to harbor endonucleolytic activity both *in vitro* and *in vivo*[37,38], suggesting that PIN domains generally may possess endonucleolytic activity.

It is well documented that NMD is tightly coupled to active translation[2,22]. Thus, the mere presence of a PTC is not sufficient for NMD to occur; instead, the recognition of a nonsense codon by translation factors is required. Premature translation termination is considerably less efficient than termination at the normal stop codon, and the consequential ribosome stalling is thought to allow the ribosome-bound UPF1 to be activated and to assemble with additional NMD factors[15]. UPF1 phosphorylation leads to the recruitment of NMD factors SMG5, SMG6 and SMG7 as well as RNA exonucleolytic activities. Whereas previous models for mammalian NMD hypothesized an ensuing attack of the RNA termini[26–29], data presented here demonstrate that the PIN domain of SMG6 promotes endonucleolytic cleavage near the PTC of the nonsense mRNA.

Whereas simultaneous knockdown of XRN1 and components of the human exosome resulted in a moderate PTC-specific increase of the β 39 reporter, wild-type TCRβ RNA was stabilized to a similar extent to the TCRβ 68 RNA under these conditions (**Supplementary Fig. 4** online). Although the β 39 result is seemingly consistent with previous notions that mammalian nonsense mRNAs can be eliminated by exonucleolysis[27–29], it is not trivial to assess the relative contribution of this pathway to NMD, as a fraction of nonsense mRNA may escape NMD and subsequently be degraded through the 'normal' exonucleolytic turnover pathway[28].

Given the currently available data, we suggest the following model for human NMD (**Fig. 5**): ribosome stalling at a PTC facilitates stable binding of UPF1 and the UPF1 kinase SMG1 to the ribosome through interaction with the release factors[39]. Subsequent interaction of UPF1 with UPF2 and UPF3 directs SMG1-mediated phosphorylation of UPF1, which in turn recruits SMG5, SMG7 and/or SMG6 (the stoichiometry of UPF1 interaction with SMG5, SMG6 and SMG7 is not known)[40–43]. Finally, this leads to SMG6-mediated endocleavage near the PTC followed by rapid exonucleolytic degradation of the cleavage products, or to alternative decay pathways involving degradation from either of the RNA termini. Although the relative contributions of endo- and exonucleolytic degradation activities to NMD may vary between substrates, data presented here identify endonucleolysis by SMG6 as an important determinant for NMD in human cells.

METHODS

Plasmids and cell lines. HeLa cells stably expressing wild-type TCRβ (pβ433), TCRβ 68 (pβ434) and Ig-μ reporter genes were described previously[31,44]. We generated pcDNA5 FRT/TO constructs containing β-globin variants and subsequently produced stable HEK293 Flp-In T-rex cell lines as previously described[45], with the exception that the BGH poly(A) site in the pcDNA5 FRT/TO vector was exchanged with the late poly(A) site from SV40. We generated 61-residue or 82-residue truncated β-globin open reading frames by introducing nonsense mutations at codons 62 (AAG to TAG) and 83 (AAG to TAG) using the QuickChange XL Site-Directed Mutagensis Kit (Stratagene). pSUPuro plasmids used in knockdown experiments were generated as described[46]. Human SMG6 (KIAA0732) cDNA was purchased from Kazusa DNA research institute, Japan. We introduced three silent mutations to change the RNAi target site from 5′-GCTGCAGGTTACTTACAAG-3′ to 5′-GCTCCAAGTTACTTATAAG-3′. Similarly, point mutations were introduced using the QuickChange Multi-Site-Directed Mutagenesis Kit (Stratagene) to generate SMG6 mutants. The ORF was then amplified by PCR and ligated into the *XbaI* site of the pcDNA3-HA vector (Invitrogen). The sequences of all plasmids were confirmed by sequencing.

RNA interference–mediated knockdowns. In HeLa-TCRβ cell lines, we carried out knockdowns using pSUPuro plasmids as described[17]. Briefly, 2×10^5 cells were seeded into a 3.5-cm plate, and the following day the cells were transfected with 200–500 ng pSUPuro plasmids using DreamFect according to the manufacturer's protocol (OZ Biosciences). The next day, 1.5 μg ml^{-1} puromycin was added for 48 h to eliminate untransfected cells. RNA and whole-cell lysates for western blotting were isolated after 24 h of further incubation in puromycin-free medium. In SMG6 knockdowns, puromycin selection (3 μg ml^{-1}) was reduced to 24 h.

For SMG6 and XRN1 double knockdown, cells were transfected with pSUPuro XRN1, and 48 h later cells were retransfected with pSUPuro XRN1, pSUPuro SMG6 and pcDNA3-HA-SMG6. Small interfering RNA

© 2008 Nature Publishing Group http://www.nature.com/nsmb

(siRNA)–mediated knockdown in the HEK293–β-globin cell lines was carried out by a previously described double-transfection procedure[47]. Briefly, 2.7×10^5 cells were seeded in a 3.5-cm plate, and the following day they were transfected with 45 pmol of siRNA using siLentFect (Bio-Rad). After 48 h, the cells were retransfected with 45 pmol of siRNA using Lipofectamine 2000 (Invitrogen). After 24 h, expression from the β-globin gene was induced by addition of tetracycline at 250 ng ml^{-1}. Protein extracts and total RNA were prepared after 24 h of further incubation.

For the experiments shown in **Figure 3c**, 4.5×10^5 cells were seeded in a 3.5-cm plate, and the following day siRNAs and plasmids were cotransfected using Lipofectamine 2000. After 72 h, the cells were retransfected with siRNA. After another 24 h, the β-globin gene was induced for 24 h before harvesting. To obtain approximately equal expression of wild-type and mutant HA-$SMG6^R$ in HEK293 cells, 0.5 μg and 4 μg, respectively, of the corresponding plasmids were used in the transfections. The siRNA target sequences for XRN1, XRN2 and DCP2 were as described[45]. Different siRNA targets were used for knockdown of UPF1 (see ref. 48 for HEK293 cells and ref. 49 for HeLa cells) and as control (see ref. 50 for HEK293: EGFP and ref. 51 for HeLa: scrambled control). Furthermore, the following factors were depleted: SMG6 (5′-GCUGCAGGU UACUUACAAG-3′); EXOSC1 (human homolog of Csl4) (5′-GAAAGUAGC CCGAGUACAA-3′); EXOSC2 (homolog of Rrp4) (5′-GGUGGAAGGUGGA GACCAA-3′); EXOSC4 (homolog of Rrp41) (5′-CUAGUGAACUGUCAA UAUA-3′); SKIV2L (homolog of Mtr4 or Ski2) (5′-GGAGAUAGACUUUGAG AAA-3′); WDR61 (homolog of Ski8) (5′-GCUCUCUUGAUGCUCAUAU-3′). Knockdown efficiencies of the various targets were verified by western blotting or RT-qPCR analysis.

RNA manipulations. Northern blotting analyses were performed according to standard procedures. Briefly, RNA (approximately 10–15 μg per sample) was separated on a 1.2% (w/v) agarose gel containing 1× MOPS and 1% (v/v) formaldehyde and transferred to a positively charged nylon membrane by wet blotting. Subsequent hybridization was done in ULTRAHyb buffer (Ambion) at 68 °C and according to the manufacturer's guidelines. Specific riboprobes were transcribed by use of the Strip-EZ RNA kit (Ambion). To distinguish 3′ fragments from full-length transcripts expanding into this region of the blot, the average of the signal intensity just above and below the region of the 3′ fragment was defined as background and subtracted from the signal intensity determined in the 3′ fragment region. Polyadenylated RNA was purified using PolyA-purist (Ambion) columns according to the manufacturer's guidelines. One-twentieth of each RNA fraction was loaded on the gel (approximately 12.5 μg for the total and unbound fractions). We carried out RT-qPCR analysis essentially as described[17,47], with amplicons situated either upstream (5′) or downstream (3′) of the PTC.

The 5′ ends of the 3′ fragments produced upon knockdown of XRN1 from the various β-globin genes with PTCs were identified by use of the 5′ RACE System for Rapid Amplification of cDNA Ends, Version 2.0 (Invitrogen). Specific β-globin cDNA was produced using the primer 5′-AGACCCA GTTTGGTAGTTGG-3′. 5′ fragments were PCR amplified using the AP primer from the kit together with the β-globin–specific primer 5′-GCACTGGTG GGGTGAATTC-3′. The produced products were re-amplified in a seminested PCR using the latter β-globin primer and the kit primer AUAP. PCR products were purified and ligated into pCR4-TOPO (Invitrogen) followed by sequencing of individual clones. RNase protection assays were carried out essentially as described previously[31].

Expression and purification of recombinant PIN domain. PIN domains (residues 1239–1421) of wild-type and mutant (D1353A) SMG6 were cloned in pGEX-6P (Amersham Pharmacia Biotech) and transformed in *E. coli* BL21-CodonPlus-RIPL. Selected transformants were grown in 1 liter LB at 37 °C, and protein expression was induced by addition of 1.0 mM IPTG at an optical density at 600 nm ($OD_{600\ nm}$) of 0.6. After a 3-h incubation, bacteria were resuspended in PBS including complete protease inhibitors (Roche) and lysed by sonication. After centrifugation, SMG6-GST fusion proteins were purified using Glutathione Sepharose (GE Healthcare) and eluted with 10 mM reduced glutathione in 50 mM Tris, pH 8.

***In vitro* cleavage.** Circular RNA was prepared by incubation of 150 pmol U_{30} ribooligonucleotide (Microsynth) with 250 pmol unlabeled ATP and 5 pmol γ^{32}P ATP in PNK buffer using T4 polynucleotide kinase and T4 RNA ligase (New England Bioloabs). Circular RNA was extracted from 20% (w/v) PAGE and 0.01 pmol was used in the cleavage assay with about approximately 500 ng protein in 20 mM HEPES, pH 7.5, 150 mM NaCl, 10% (v/v) glycerol and 1 mM DTT at 30 °C. Reaction products were resolved on 20% (w/v) PAGE.

Note: Supplementary information is available on the Nature Structural & Molecular Biology website.

ACKNOWLEDGMENTS

We thank J. Lykke-Andersen (University of Colorado, USA), G. Pruijn (Radboud University Nijmegen, The Netherlands), J. Lingner (Ecole Polytechnique Federale de Lausanne, Switzerland), M.-D. Ruepp and D. Schümperli (both University of Bern, Switzerland) for reagents; J. Lykke-Andersen and M. Rosbash for comments on the manuscript; and D. Riishøj and K. Jürgensen for excellent technical assistance. B. Seraphin and A. Dziembowski are acknowledged for communication of unpublished results. The work was supported by the Danish National Research Foundation and the Danish Natural Science Research Council (S.L.-A. and T.H.J.), and by the Swiss National Science Foundation, the Max Cloëtta Foundation and a Starting Grant of the European Research Council (A.B.E. and O.M.).

Published online at http://www.nature.com/nsmb/
Reprints and permissions information is available online at http://npg.nature.com/reprintsandpermissions/

1. Doma, M.K. & Parker, R. RNA quality control in eukaryotes. *Cell* **131**, 660–668 (2007).
2. Amrani, N., Sachs, M.S. & Jacobson, A. Early nonsense: mRNA decay solves a translational problem. *Nat. Rev. Mol. Cell Biol.* **7**, 415–425 (2006).
3. Behm-Ansmant, I. *et al.* mRNA quality control: an ancient machinery recognizes and degrades mRNAs with nonsense codons. *FEBS Lett.* **581**, 2845–2853 (2007).
4. Isken, O. & Maquat, L.E. Quality control of eukaryotic mRNA: safeguarding cells from abnormal mRNA function. *Genes Dev.* **21**, 1833–1856 (2007).
5. Muhlemann, O., Eberle, A.B., Stalder, L. & Zamudio Orozco, R. Recognition and elimination of nonsense mRNA. *Biochim. Biophys. Acta* **1779**, 538–549 (2008).
6. Lewis, B.P., Green, R.E. & Brenner, S.E. Evidence for the widespread coupling of alternative splicing and nonsense-mediated mRNA decay in humans. *Proc. Natl. Acad. Sci. USA* **100**, 189–192 (2003).
7. Rehwinkel, J., Raes, J. & Izaurralde, E. Nonsense-mediated mRNA decay: target genes and functional diversification of effectors. *Trends Biochem. Sci.* **31**, 639–646 (2006).
8. Stalder, L. & Muhlemann, O. The meaning of nonsense. *Trends Cell Biol.* **18**, 315–321 (2008).
9. He, F. *et al.* Genome-wide analysis of mRNAs regulated by the nonsense-mediated and 5′ to 3′ mRNA decay pathways in yeast. *Mol. Cell* **12**, 1439–1452 (2003).
10. Mendell, J.T., Sharifi, N.A., Meyers, J.L., Martinez-Murillo, F. & Dietz, H.C. Nonsense surveillance regulates expression of diverse classes of mammalian transcripts and mutes genomic noise. *Nat. Genet.* **36**, 1073–1078 (2004).
11. Rehwinkel, J., Letunic, I., Raes, J., Bork, P. & Izaurralde, E. Nonsense-mediated mRNA decay factors act in concert to regulate common mRNA targets. *RNA* **11**, 1530–1544 (2005).
12. Wittmann, J., Hol, E.M. & Jack, H.M. hUPF2 silencing identifies physiologic substrates of mammalian nonsense-mediated mRNA decay. *Mol. Cell. Biol.* **26**, 1272–1287 (2006).
13. Johansson, M.J., He, F., Spatrick, P., Li, C. & Jacobson, A. Association of yeast Upf1p with direct substrates of the NMD pathway. *Proc. Natl. Acad. Sci. USA* **104**, 20872–20877 (2007).
14. Holbrook, J.A., Neu-Yilik, G., Hentze, M.W. & Kulozik, A.E. Nonsense-mediated decay approaches the clinic. *Nat. Genet.* **36**, 801–808 (2004).
15. Amrani, N. *et al.* A faux 3′-UTR promotes aberrant termination and triggers nonsense-mediated mRNA decay. *Nature* **432**, 112–118 (2004).
16. Behm-Ansmant, I., Gatfield, D., Rehwinkel, J., Hilgers, V. & Izaurralde, E. A conserved role for cytoplasmic poly(A)-binding protein 1 (PABPC1) in nonsense-mediated mRNA decay. *EMBO J.* **26**, 1591–1601 (2007).
17. Eberle, A.B., Stalder, L., Mathys, H., Zamudio Orozco, R. & Muhlemann, O. Post-transcriptional gene regulation by spatial rearrangement of the 3′ untranslated region. *PLoS Biol.* **6**, e92 (2008).
18. Ivanov, P.V., Gehring, N.H., Kunz, J.B., Hentze, M.W. & Kulozik, A.E. Interactions between UPF1, eRFs, PABP and the exon junction complex suggest an integrated model for mammalian NMD pathways. *EMBO J.* **27**, 736–747 (2008).
19. Longman, D., Plasterk, R.H., Johnstone, I.L. & Caceres, J.F. Mechanistic insights and identification of two novel factors in the *C. elegans* NMD pathway. *Genes Dev.* **21**, 1075–1085 (2007).
20. Silva, A.L., Ribeiro, P., Inacio, A., Liebhaber, S.A. & Romao, L. Proximity of the poly(A)-binding protein to a premature termination codon inhibits mammalian nonsense-mediated mRNA decay. *RNA* **14**, 563–576 (2008).

© 2008 Nature Publishing Group http://www.nature.com/nsmb

21. Singh, G., Rebbapragada, I. & Lykke-Andersen, J. A competition between stimulators and antagonists of Upf complex recruitment governs human nonsense-mediated mRNA decay. *PLoS Biol.* **6**, e111 (2008).
22. Thermann, R. *et al.* Binary specification of nonsense codons by splicing and cytoplasmic translation. *EMBO J.* **17**, 3484–3494 (1998).
23. Cao, D. & Parker, R. Computational modeling and experimental analysis of nonsense-mediated decay in yeast. *Cell* **113**, 533–545 (2003).
24. Hagan, K.W., Ruiz-Echevarria, M.J., Quan, Y. & Peltz, S.W. Characterization of *cis*-acting sequences and decay intermediates involved in nonsense-mediated mRNA turnover. *Mol. Cell. Biol.* **15**, 809–823 (1995).
25. Muhlrad, D. & Parker, R. Premature translational termination triggers mRNA decapping. *Nature* **370**, 578–581 (1994).
26. Chen, C.Y. & Shyu, A.B. Rapid deadenylation triggered by a nonsense codon precedes decay of the RNA body in a mammalian cytoplasmic nonsense-mediated decay pathway. *Mol. Cell. Biol.* **23**, 4805–4813 (2003).
27. Couttet, P. & Grange, T. Premature termination codons enhance mRNA decapping in human cells. *Nucleic Acids Res.* **32**, 488–494 (2004).
28. Lejeune, F., Li, X. & Maquat, L.E. Nonsense-mediated mRNA decay in mammalian cells involves decapping, deadenylating, and exonucleolytic activities. *Mol. Cell* **12**, 675–687 (2003).
29. Yamashita, A. *et al.* Concerted action of poly(A) nucleases and decapping enzyme in mammalian mRNA turnover. *Nat. Struct. Mol. Biol.* **12**, 1054–1063 (2005).
30. Gatfield, D. & Izaurralde, E. Nonsense-mediated messenger RNA decay is initiated by endonucleolytic cleavage in *Drosophila*. *Nature* **429**, 575–578 (2004).
31. Mohn, F., Buhler, M. & Muhlemann, O. Nonsense-associated alternative splicing of T-cell receptor β genes: no evidence for frame dependence. *RNA* **11**, 147–156 (2005).
32. Stoecklin, G., Stoeckle, P., Lu, M., Muehlemann, O. & Moroni, C. Cellular mutants define a common mRNA degradation pathway targeting cytokine AU-rich elements. *RNA* **7**, 1578–1588 (2001).
33. Kammler, S., Lykke-Andersen, S. & Jensen, T.H. The RNA exosome component hRrp6 is a target for 5-fluorouracil in human cells. *Mol. Cancer Res.* **6**, 990–995 (2008).
34. Clissold, P.M. & Ponting, C.P. PIN domains in nonsense-mediated mRNA decay and RNAi. *Curr. Biol.* **10**, R888–R890 (2000).
35. Glavan, F., Behm-Ansmant, I., Izaurralde, E. & Conti, E. Structures of the PIN domains of SMG6 and SMG5 reveal a nuclease within the mRNA surveillance complex. *EMBO J.* **25**, 5117–5125 (2006).
36. Huntzinger, E., Kashima, I., Fauser, M., Sauliere, J. & Izaurralde, E. SMG6 is the catalytic endonuclease that cleaves mRNAs containing nonsense codons in metazoan. *RNA* published online doi:10.1261/rna.1386208 (30 October 2008).
37. Lebreton, A., Tomecki, R., Dziembowski, A. & Séraphin, B. Endonucleolytic RNA cleavage by a eukaryotic exosome. *Nature* advance online publication, doi:10.1038/nature07480 (7 December 2008).
38. Schaeffer, D. *et al.* The exosome contains domains with specific endoribonuclease, exoribonuclease and cytoplasmic mRNA decay activities. *Nat. Struct. Mol. Biol.* advance online publication, doi:10.1038/nsmb.1528 (7 December 2008).
39. Kashima, I. *et al.* Binding of a novel SMG-1-Upf1-eRF1-eRF3 complex (SURF) to the exon junction complex triggers Upf1 phosphorylation and nonsense-mediated mRNA decay. *Genes Dev.* **20**, 355–367 (2006).
40. Anders, K.R., Grimson, A. & Anderson, P. SMG-5, required for *C. elegans* nonsense-mediated mRNA decay, associates with SMG-2 and protein phosphatase 2A. *EMBO J.* **22**, 641–650 (2003).
41. Chiu, S.Y., Serin, G., Ohara, O. & Maquat, L.E. Characterization of human Smg5/7a: a protein with similarities to *Caenorhabditis elegans* SMG5 and SMG7 that functions in the dephosphorylation of Upf1. *RNA* **9**, 77–87 (2003).
42. Fukuhara, N. *et al.* SMG7 is a 14–3-3-like adaptor in the nonsense-mediated mRNA decay pathway. *Mol. Cell* **17**, 537–547 (2005).
43. Ohnishi, T. *et al.* Phosphorylation of hUPF1 induces formation of mRNA surveillance complexes containing hSMG-5 and hSMG-7. *Mol. Cell* **12**, 1187–1200 (2003).
44. Buhler, M., Paillusson, A. & Muhlemann, O. Efficient downregulation of immunoglobulin μ mRNA with premature translation-termination codons requires the 5′-half of the VDJ exon. *Nucleic Acids Res.* **32**, 3304–3315 (2004).
45. Damgaard, C.K. *et al.* A 5′ splice site enhances the recruitment of basal transcription initiation factors *in vivo*. *Mol. Cell* **29**, 271–278 (2008).
46. Brummelkamp, T.R., Bernards, R. & Agami, R. A system for stable expression of short interfering RNAs in mammalian cells. *Science* **296**, 550–553 (2002).
47. Lykke-Andersen, S., Pinol-Roma, S. & Kjems, J. Alternative splicing of the ADAR1 transcript in a region that functions either as a 5′-UTR or an ORF. *RNA* **13**, 1732–1744 (2007).
48. Mendell, J.T., ap Rhys, C.M. & Dietz, H.C. Separable roles for rent1/hUpf1 in altered splicing and decay of nonsense transcripts. *Science* **298**, 419–422 (2002).
49. Paillusson, A., Hirschi, N., Vallan, C., Azzalin, C.M. & Muhlemann, O. A GFP-based reporter system to monitor nonsense-mediated mRNA decay. *Nucleic Acids Res.* **33**, e54 (2005).
50. Lewis, D.L., Hagstrom, J.E., Loomis, A.G., Wolff, J.A. & Herweijer, H. Efficient delivery of siRNA for inhibition of gene expression in postnatal mice. *Nat. Genet.* **32**, 107–108 (2002).
51. Buhler, M., Steiner, S., Mohn, F., Paillusson, A. & Muhlemann, O. EJC-independent degradation of nonsense immunoglobulin-μ mRNA depends on 3′ UTR length. *Nat. Struct. Mol. Biol.* **13**, 462–464 (2006).

© 2008 Nature Publishing Group http://www.nature.com/nsmb

Supplementary Figure 1

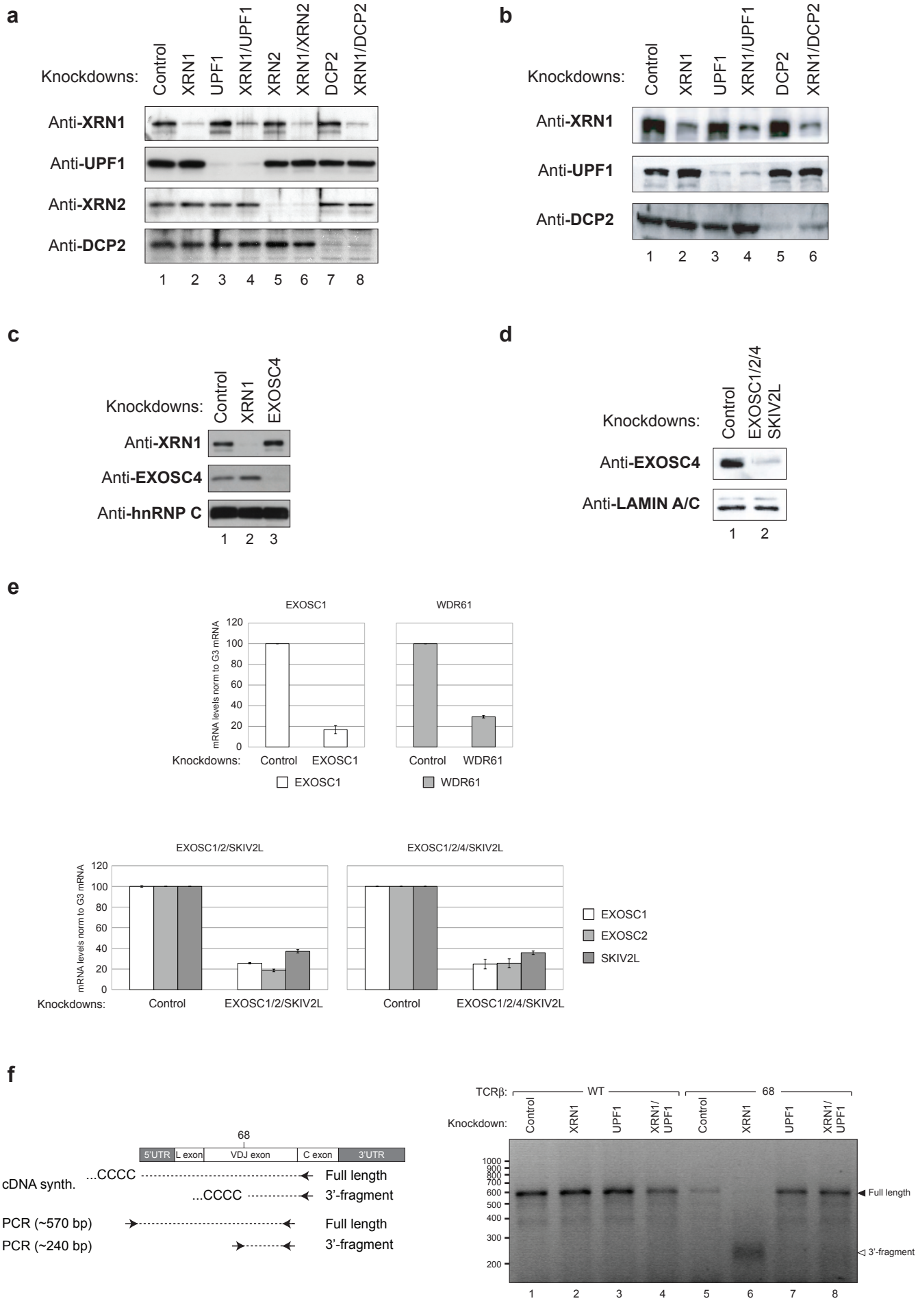

Supplementary Figure 1. a-e, Knockdown efficiencies analyzed by Western blotting analyses or RT-qPCR. Western blotting analysis of HEK293 (**a, c**) and HeLa (**b, d**) cell lysates for XRN1, UPF1, XRN2, DCP2, and EXOSC4 depletions. hnRNP C (**c**) and LAMIN A/C (**d**) served as loading controls. **e,** RT-qPCR of total RNA harvested from HeLa cells depleted for the indicated factors. Mean values of EXOSC1, WDR61, EXOSC2, and SKIV2L mRNA levels (normalised to GAPDH mRNA) with standard deviations were calculated (n=3). **a**-**b** corresponds to the experiments shown in **Fig. 1c-d**, and **c**-**e** corresponds to the experiments shown in **Fig. 1f-g**. **f,** (*left*) schematic illustration of the 5'RACE analysis of TCRβ RNA. Expected sizes of the PCR products for full length mRNA and the 3' fragment are given in brackets next to the respective fragments. The expected size of the 3'-fragment is based on the position of the PTC. (*right*) Ethidium bromide stained agarose gel showing the PCR products obtained from the 5'-RACE procedure on RNA samples corresponding to those shown in **Fig. 1d**, lanes 1-4 and 7-10.

Supplementary Figure 2

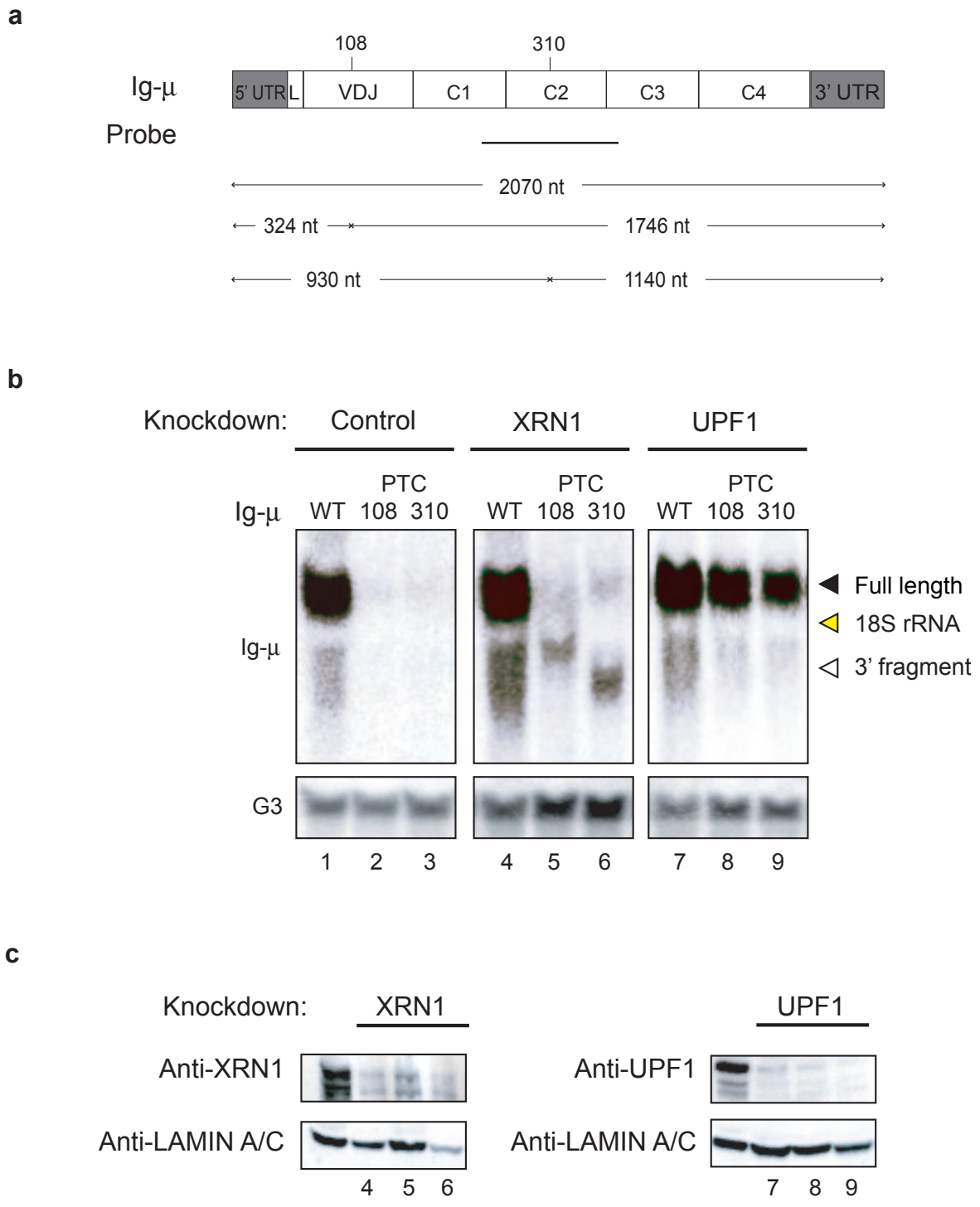

Supplementary Figure 2. Detection of 3' fragments of Ig-μ nonsense mRNAs upon depletion of XRN1. **a,** schematic representation of Ig-μ mRNA with PTCs at amino acid positions 108 and 310. The position of the Northern probe and the predicted length of endo-cleaved products are shown. **b**, Northern blotting analysis of total RNA isolated from HeLa-Ig-μ wt/PTC108/PTC310 cell lines depleted for the indicated factors. GAPDH (G3) levels served as loading control. **c**, Western blotting analysis monitoring efficiencies of XRN1 and UPF1 knockdowns. Lamin A/C served as loading control.

Supplementary Figure 3

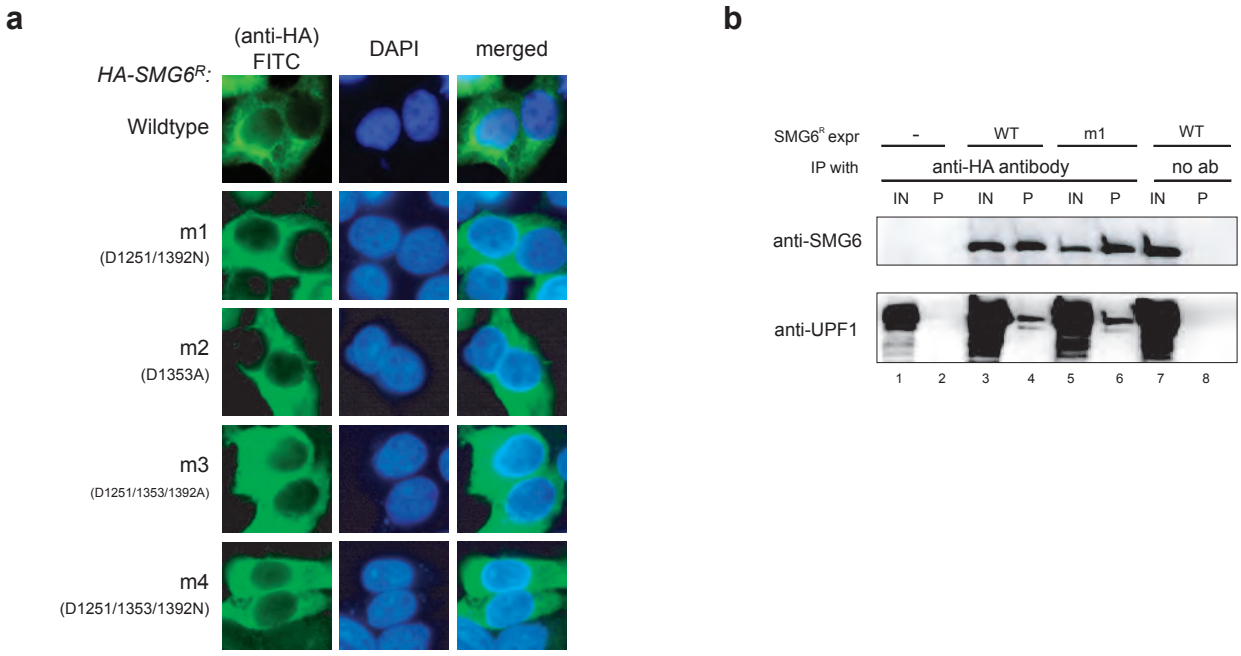

Supplementary Figure 3. a, Immunofluorescent localization analyses of HA-SMG6^R variants transiently expressed in HEK293 cells using a rat anti-HA primary antibody followed by a FITC-conjugated goat-anti-rat secondary antibody. Nuclei were stained with DAPI and images were overlayed as indicated. Untransfected cells displayed only a modest background staining, which was dispersed all over the cells (not shown). **b**, Co-immunoprecipitation of HA-SMG6^R variants using an anti-HA antibody. The samples were treated with RNase A and 1/100 of the cell lysate was used as input. Immunoprecipitates were analysed by Western blotting using antibodies against SMG6 and UPF1.

Supplementary Figure 4

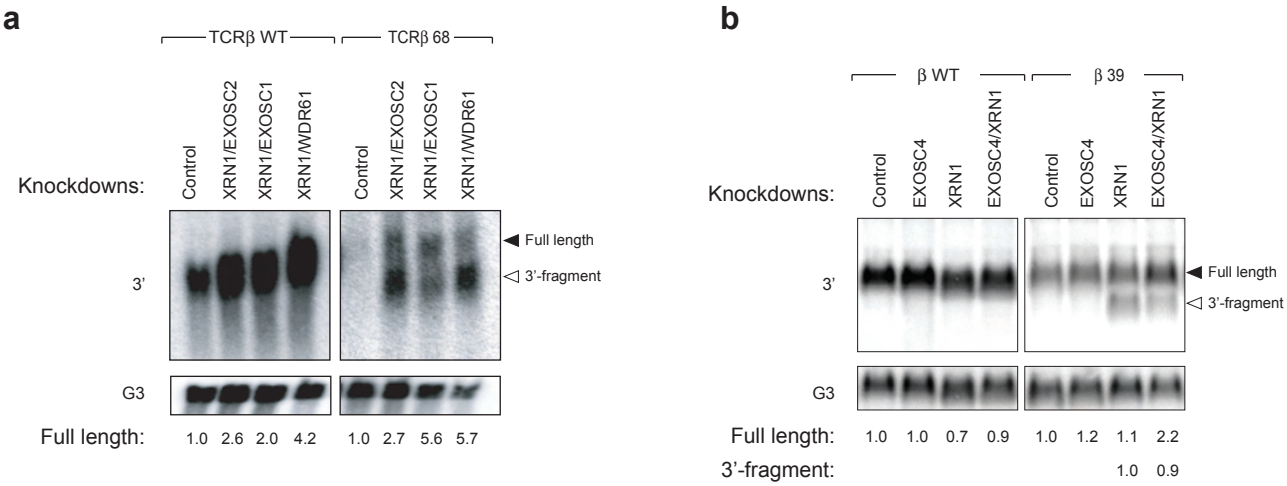

Supplementary Figure 4. Northern blotting analysis of total RNA isolated from HeLa-TCRβ wt/68 (**a**) and HEK293-β-globin wt/39 **(b)** cells depleted for the indicated 3'-5'- and 5'-3'-exonucleolytic factors. Blots were hybridized with probes directed against the 3'- regions of the respective reporter RNAs as described in **Fig. 1c-d**. GAPDH (G3) levels were detected as an internal loading standard. Quantification of selected signals can be seen below the blots.

Supplementary Information

SUPPLEMENTARY METHODS

Co-immunoprecipitation. HeLa cells overexpressing HA-SMG6 and UPF1 were harvested after 2 days, washed in PBS, and lysed for 3 min in 10 mM HEPES (pH 7.9), 100 mM KCl, 1 mM EDTA, 1 mM DTT, 0.5 % (v/v) NP-40, and 1x complete protease inhibitors (Roche) on ice. After centrifugation (4500g, 1 min, 4 °C), supernatants were incubated with 40 μg RNAse A for 10 min on ice. Protein-G-sepharose-beads (GE Healthcare), which were coupled over night with 5 μg HA-antibodies (Roche), were added to the cell lysates. After 3 hours on a turning wheel at 4 °C, beads were washed 5 times with 10 mM Tris-HCl, pH7.5, 150 mM NaCl, 0.1 % (v/v) NP-40. Immunoprecipitation products were separated by SDS-PAGE followed by Western blotting.

Immunolocalizaion analysis. Immunofluorescent staining of HEK293 cells transiently expressing HA-SMG6^{R} WT and mutant variants was done by standard procedure. Cells grown on coverslips (pre-treated with poly-(L)-lysine) were fixed in PBS containing 4% (w/v) paraformaldehyde, permeabilized in PBS containing 0.1% (v/v) Triton X-100 and then incubated over night at 4°C with a primary antibody against HA (rat anti-HA high affinity antibody, Roche, 1:40) followed by 1 hour incubation at room temperature with a FITC-conjugated goat-anti-rat antibody (Sigma, 1:250). Cells were mounted in DAPI solution and analyzed on an Olympus BX51 microscope equipped with a cooled Olympus DP50 CCD camera and analySIS software.